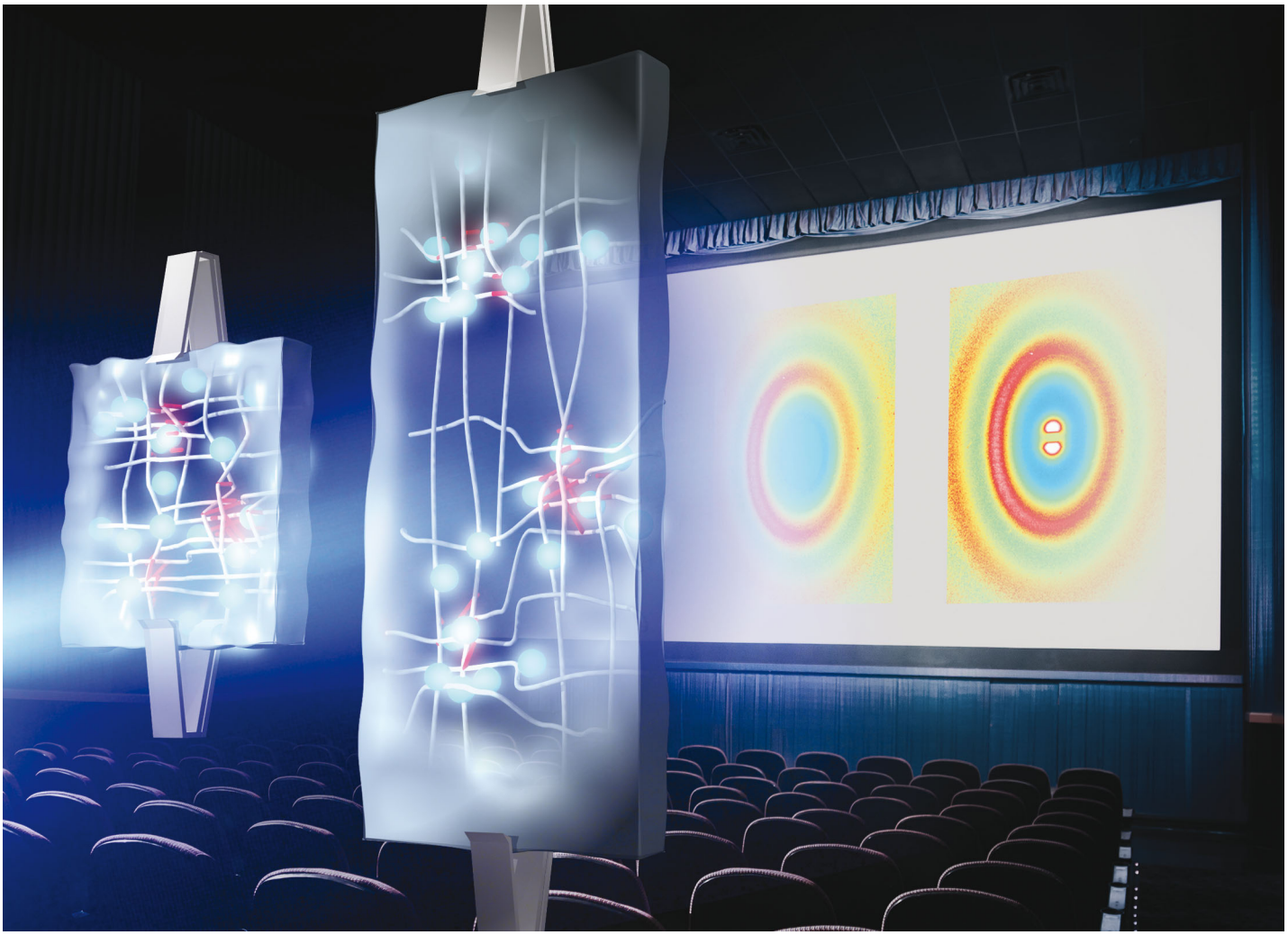

Highlighting research results from Georg-August-Universität, Germany and the University of Tokyo, Japan.

Probe-SAXS on hydrogels under elongation

In order to evaluate the cross-linking inhomogeneity in polymer networks, we introduced nano-particles which do not interact with polymers and conducted SAXS under elongation. We succeeded in observing the sharp correlation peak of the high cross-linking region.

As featured in:

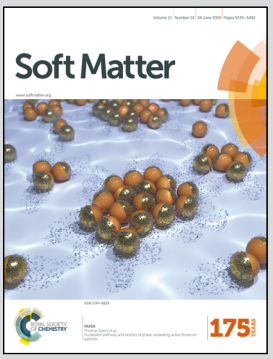

See Kengo Nishi and Mitsuhiro Shibayama, *Soft Matter*, 2016, **12**, 5334.

ROYAL SOCIETY OF CHEMISTRY

www.softmatter.org

Registered charity number: 207890

Soft Matter

PAPER

View Article Online
View Journal | View Issue

Cite this: *Soft Matter*, 2016, **12**, 5334

Probe-SAXS on hydrogels under elongation†

Kengo Nishi‡*[a] and Mitsuhiro Shibayama§*[b]

Received 8th March 2016,
Accepted 29th April 2016

DOI: 10.1039/c6sm00591h

www.rsc.org/softmatter

We have investigated the effect of polymer/filler interaction on the displacements of silica nanoparticles in gels by introducing them into poly(*N*,*N*-dimethylacrylamide) gel (PDAM-NP gel) and polyacrylamide gel (PAM-NP gel). It is well known that PDAM chains are strongly adsorbed onto silica nanoparticles, while PAM chains are not. We carried out SAXS measurements on these gels under uniaxial elongation. Interestingly, we found that the SAXS scattering profiles of PDAM-NP and PAM-NP gels were totally different. A four-spot pattern was observed in the 2D structure factors of the PDAM-NP gel and was assigned to the movement of the nanoparticles in an affine way. On the other hand, as for the PAM-NP gel, a sharp peak was observed in the much lower q region than the prediction of affine deformation, indicating that the peak corresponds to the correlation peak of the high cross-linking region. These experimental findings may lead to the development of "probe-SAXS", which is a new technology for detecting nano-order inhomogeneity in hydrogels.

1 Introduction

Hydrogels are soft elastic solids and contain a large portion of water. By taking advantage of the high water absorption and elastic properties, hydrogels are applied to many kinds of industrial products such as diapers, drug reservoirs, and contact lenses. Though hydrogels have these characteristic properties, their industrial application is still limited due to their low mechanical strength. Because this low mechanical strength is related to cross-linking inhomogeneity, the relationship between the network structure and mechanical properties has been investigated in order to toughen hydrogels by scattering experiments,[1–3] AFM,[4–6] microrheology,[7–9] and other techniques.[10,11] However, this relationship is still unrevealed because no decisive method for detecting the inhomogeneity is well-established.

One of the most effective methods to enhance the mechanical properties of inhomogeneous hydrogels is the introduction of fillers to polymeric materials such as carbon blacks,[12] silica particles,[13] carbon nanotubes[14,15] and inorganic clays.[16] It is well known that the mechanical performance is remarkably enhanced by the introduction of fillers because of the interaction between fillers and polymers. Therefore, a proper and better understanding of the interaction between fillers and polymers is necessary not only from a basic science point of view but also from an industrial point of view.

Among the above mentioned fillers, hydrogels with silica nanoparticles offer a distinct advantage of simplicity to study the filler effect on mechanical properties. Because of their simplicity, nanocomposite hydrogels with silica nanoparticles have been well studied.[17–24] Lin *et al.* and Rose *et al.* showed an enhancement of mechanical properties by introducing silica nanoparticles into poly(*N*,*N*-dimethylacrylamide) (PDAM) gel.[17,18,21] On the other hand, Lin *et al.* also reported that the introduction of silica nanoparticles into the polyacrylamide (PAM) gel does not lead to any significant reinforcement in the mechanical properties in contrast to the PDAM gel.[19] This difference seems to be ascribed to the difference in the adsorption of polymers onto silica nanoparticles. Rose *et al.* introduced silica nanoparticles into the P(AM-*co*-DAM) gel and investigated the interaction between the polymer and silica nanoparticles.[22] Using dynamic scattering experiments, they showed that there existed an adsorption layer of PDAM onto silica nanoparticles, while no adsorption of PAM occurred. However, it remains unclear how the difference in the polymer/filler interaction affects the deformation mechanism of nanocomposite hydrogels. We believe that it is important to know the effect of the difference in the polymer/filler interaction on the internal structure of nanocomposite hydrogels in order to understand the filler effect.

Thus, in this study, we conducted small-angle X-ray scattering on PDAM-NP and PAM-NP gels under elongation to elucidate the effect of polymer/filler interaction on the deformation mechanism of nanocomposite gels. In SAXS experiments, we found that the SAXS scattering profiles of PDAM-NP and PAM-NP gels are

[a] *Third Institute of Physics-Biophysics, Georg August University, 37077 Goettingen, Germany. E-mail: kengo.nishi@phys.uni-goettingen.de*
[b] *Institute for Solid State Physics, The University of Tokyo, 5-1-5 Kashiwanoha, Kashiwa, Chiba 277-8581, Japan. E-mail: sibayama@issp.u-tokyo.ac.jp*

† Electronic supplementary information (ESI) available. See DOI: 10.1039/c6sm00591h

‡ K. N. initiated and conceived the project, designed and conducted the experiments, interpreted the results, and wrote the manuscript.

§ M. S. gave a general discussion, supervised the project and also wrote the manuscript.

totally different. Furthermore, we unexpectedly observed a sharp peak for the PAM-NP gel in the very low-q region, which may correspond to cross-linking inhomogeneity.

2 Experiment

2.1 Materials

Acrylamide (AM, Wako), *N*,*N*-dimethylacrylamide (DAM, Wako), potassium persulfate (KPS, Sigma Aldrich), *N*,*N*,*N*′,*N*′-tetramethylethylenediamine (TEMED, Sigma-Aldrich), and *N*,*N*′-methylenebis-(acrylamide) (BIS, Sigma Aldrich) were used as received. Silica nanoparticles (Ludox TM-50 from Dupont) were obtained from Sigma Aldrich. In our preliminary SAXS experiments on a dilute solution of TM-50, the mean radius of nanoparticles was estimated to be $\sim$130 Å.

2.2 Sample preparation

The compositions of the hydrogels are summarized in Table 1. The molar ratio of monomer to [TEMED] and to [KPS] was fixed at 100/1. The cross-linking density was also kept constant as a cross-linker/monomer molar ratio of 3 M/1.5 mM. The amount of silica particles was fixed at 20 wt%. A certain amount of KPS was dissolved in 2 ml deionized water. Separately, certain amounts of silica suspension, monomer, TEMED and BIS were dissolved in a certain amount of water. All solutions were deoxygenated by bubbling nitrogen for 15 min and degassed by vacuuming. This vacuum state was maintained just until initiating free-radical polymerization. The polymerization was initiated by mixing two solutions under nitrogen conditions at room temperature and the mixture was transferred into fluorine-containing rubber molds which have a dumbbell shape standardized as JIS K 6261-7 sizes (1 mm thick).

2.3 SAXS experiments

SAXS measurements were carried out at the BL03XU beamline (Frontier Softmaterial Beamline (FSBL)) at SPring-8 that is located in Sayo, Hyogo, Japan. For the PDAM-NP gel, a monochromated X-ray beam with a wavelength (λ) of 1.5 Å was used to irradiate the samples at room temperature, and the sample-to-detector distance was set at 4 m. The scattered X-rays were counted using an imaging plate detector (R-AXIS VII++, Rigaku Corporation, Japan) with 3000 × 3000 pixel arrays and a pixel size of 0.1 mm pixel^{-1}. For the PAM-NP gel with TM-50, we used X-ray beams with a wavelength (λ) of 1.0 Å and 1.5 Å for the imaging plate detector and a CCD camera, respectively. In each measurement, the samples were placed on a uniaxial stretching machine, where the sample strain was measured.

In general, the SAXS intensity of particle systems is described by[25]

$$I(\vec{q}) = I_0 P(\vec{q}) S(\vec{q}) \quad (1)$$

Table 1 Composition of nanocomposite hydrogels

Sample name	Silica weight fraction	w_{water}/g	w_{silica}/g	w_{MBA}/g	$w_{monomer}$/g
PAM-NP gel	0.2	10	4.63	2.3	2.132
PDAM-NP gel	0.2	10	4.33	2.3	2.974

where I_0, $\vec{q}$, $P(\vec{q})$, and $S(\vec{q})$ are the zero-angle scattering intensity, the scattering vector, the form factor and the structure factor, respectively. Note that scattering intensities of nanocomposite gels are more than 100 times higher than that of pure hydrogels without nanoparticles because the scattering length density of silica nanoparticles is much larger than that of polymers (data not shown). Thus, we assumed that scattering from polymers is negligibly small in the scattering profiles of nanocomposite gels and only silica particles contribute to the scattering profiles of nanocomposite hydrogels. On the basis of these results, in order to obtain the structure factors of gels, we carried out SAXS experiments on a dilute solution of nanoparticles and the scattering profiles of nanocomposite gels were divided by that of the dilute solution of nanoparticles followed by the multiplying by a normalized constant so as to meet $S(\vec{q}) = 1$ in the high-q region.

3 Results and discussions

Let us start from the SAXS data of PAM-NP and PDAM-NP gels in an unstretched state. The structure factors for PAM-NP and PDAM-NP gels in the unstretched state are shown in Fig. 1(a). The 2D scattering profiles are shown in the insets. In order to evaluate the pair distribution function (PDF), we cut the data in the low-q region and put the constant values based on extrapolation of structure factors. This treatment corresponds to the removal of parasitic scattering or disregard large aggregation which is out of our experimental range. As shown in Fig. 1(a), the structure factor of the PAM-NP gel is very different from that of the PDAM-NP gel. We calculated the PDFs for gels from the above structure factors in order to analyze the distribution of nanoparticles in gels by using the following equation.[26]

$$g(r) = 1 + \frac{1}{2\pi^2 r \rho_0}\int_0^\infty \mathrm{d}q\, q(S(q) - 1)\sin(qr)\exp\left(-\frac{q^2}{2\sigma^2}\right) \quad (2)$$

Here, ρ_0 is the number density of nanoparticles. The last exponential term is a window function to remove the termination ripples. σ is the standard deviation and we set this value as $\sigma = q_{max}/2$ by following the previous work.[26] The PDFs of PAM-NP and PDAM-NP gels are shown in Fig. 1(b). We observed large positive and negative values in PDFs near $r = 0$, which seems to be derived from the finite q-range in experimental data. In the case of the PDAM-NP gel, we observed two peaks at 250 Å and 440 Å. When we take into account the fact that the radius of nanoparticles is $\sim$130 Å, the peak at 250 Å indicates that some nanoparticles are in direct contact with each other. The peak at 440 Å may correspond to the distances between nanoparticles which are homogeneously dispersed. As for the PAM-NP gel, a strong peak can be observed at 300 Å. If we assumed that all nanoparticles are homogeneously dispersed in the gel, the distance between nearest neighbor particles is calculated to be 306 Å. Thus, this result indicates that nanoparticles in the PAM-NP gel are homogeneously dispersed in the system without disturbing the system, such as local aggregation due to depletion condensation, and the peak at 300 Å corresponds to the distance between nearest neighbor particles.

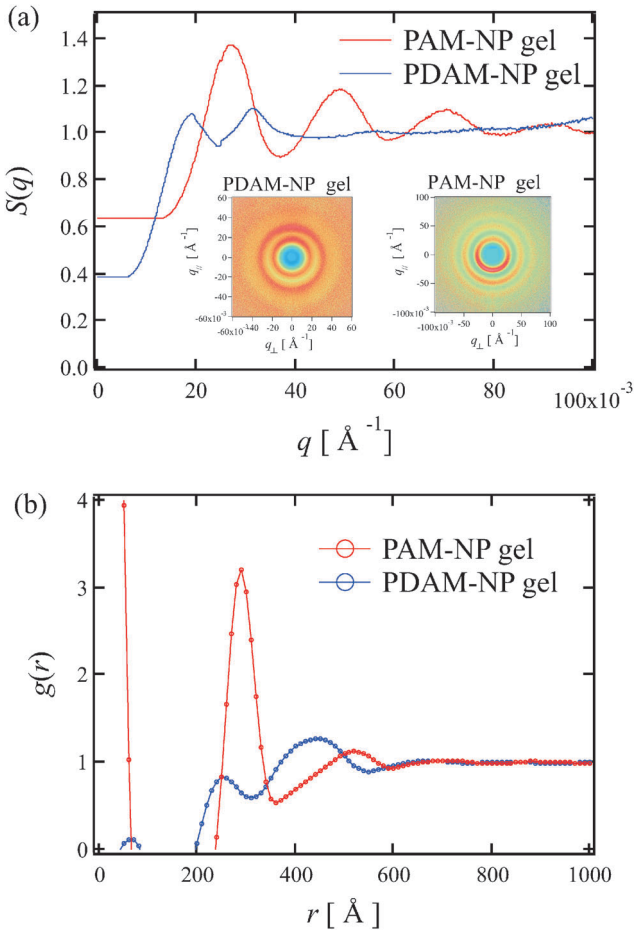

Fig. 1 (a) 1D plot of structure factors for unstretched gels. The 2D scattering intensity profiles are shown in the insets. (b) The pair distribution function (PDF) for unstretched gels. The PDF was evaluated from the structure factors using eqn (2).

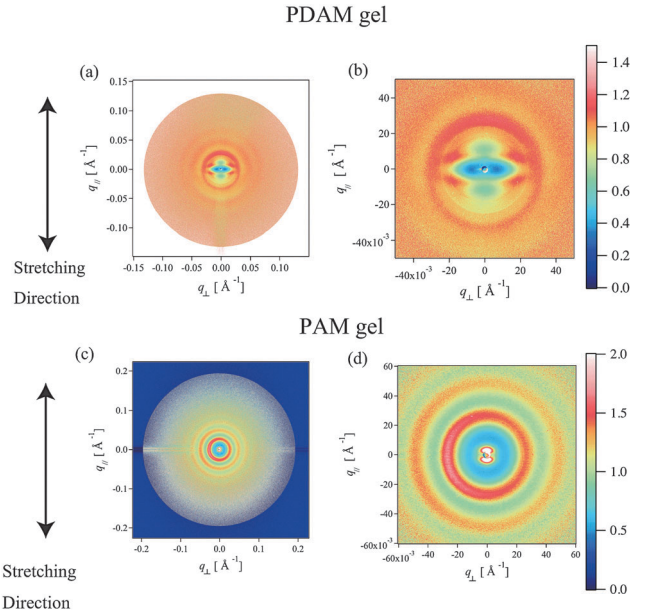

Fig. 2 2D structure factors of gels. (a) 2D structure factors of the PDAM-NP gel at λ = 2.03. (b) A magnified view of (a) in the vicinity of the beam center. (c) 2D structure factors of the PAM-NP gel at λ = 1.29. (d) A magnified view of (c) in the vicinity of the beam center.

The 2D structure factors of the PDAM-NP gel for stretched states are plotted in Fig. 2(a). An anisotropic structure factor is observed when the gel is stretched. In order to show the low-q region in detail, a magnified figure of Fig. 2(a) is plotted in the vicinity of the beam center in Fig. 2(b). As shown in Fig. 2(b), we observed a four-spot pattern. Rose *et al.* conducted SANS experiments in detail on a system (PDAM-NP gel) similar to our work.[21] However, they did not observe such a four-spot pattern but an "abnormal butterfly pattern". This difference may be ascribed to the fact that the polymer concentration of the PDAM-NP gel in the previous work[21] was half that of our experiment and the four-spot pattern was frequently observed in polymer-rich nanocomposite polymer networks such as elastomers and rubbers.[27–30] As discussed in previous work,[27–30] with regard to the origin of this four-spot pattern it is considered that some long aggregates buckle under the lateral compression, or the space in the direction perpendicular to the stretching between two aggregates is filled up by another aggregate that is forced between them.[27] On the other hand, the 2D structure factors of the PAM-NP gel (λ = 1.29) are completely different from those of the PDAM-NP gel as shown in Fig. 2(c). Note that we use X-rays with a wavelength of 1.0 Å for obtaining these results. In the intermediate range, we observed a symmetric ring pattern. In the vicinity of the low-q limit, on the other hand, we could not observe a four-spot pattern, but two-spot patterns in Fig. 2(d), which is a magnified figure of Fig. 2(c) in the vicinity of beam center. These peaks seem to appear in the much lower q-region than the theoretical prediction of affine deformation of nanoparticles. In addition, we observed similar two-spot patterns by using a different type of silica nanopaticles as discussed in Fig. S1 (ESI†). These results indicate that these two-spot patterns are highly reproducible and can be observed regardless of the type of silica nanoparticles and reflect the network structure of the PAM gel itself.

In order to discuss the sharp peaks in detail, we carried out SAXS measurements on a stretched PAM-NP gel using X-rays with a wavelength of 1.5 Å (Fig. 3). The sharp peaks can be observed more clearly than Fig. 2(d). Fig. 3(b) shows the slice images of the 2D structure factors of the PAM-NP gel at different stretching ratios in the direction parallel to the stretching. As shown in Fig. 3(b), the peak becomes more intense and the q-values of peak tops $q_{y,\mathrm{peak}}$ decrease as the stretching ratio increases. These results suggest that the distance between nanoparticles becomes systematically larger as the stretching ratio increases.

We evaluated the distances between nanoparticles (d_{peak}) from the peak position ($q_{y,\mathrm{peak}}$) in the low-q region, such as $d_{\mathrm{peak}} = 2\pi/q_{y,\mathrm{peak}}$. The solid and dotted lines shown in Fig. 4 are theoretical lines calculated for affine deformation in the direction parallel to the stretching for PAM-NP and PDAM-NP gels, respectively. As for the evaluation of $q_{y,\mathrm{peak}}$ for the PDAM-NP gel, we focused on the distance between nanoparticles which are not directly attached to each other and homogeneously dispersed

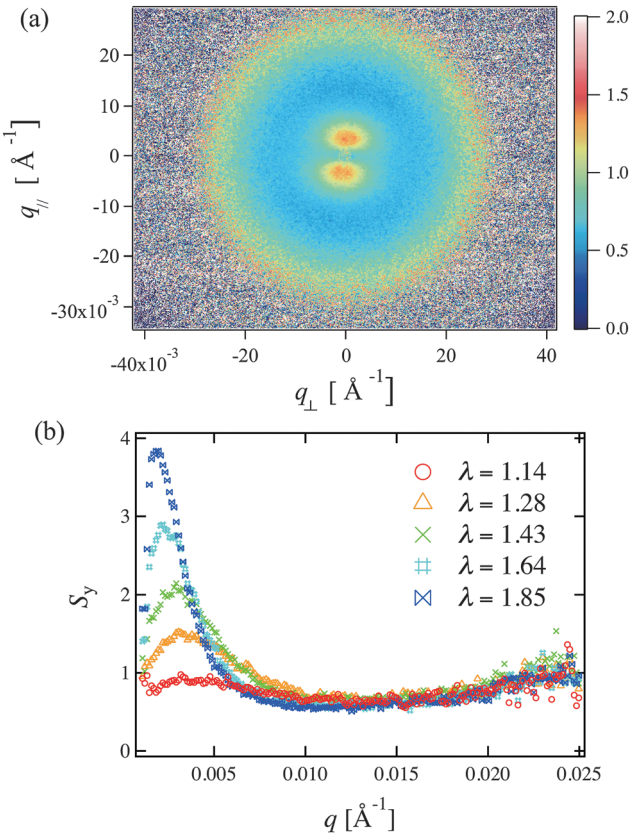

Fig. 3 (a) 2D structure factors of the PAM-NP gel at λ = 1.28. This pattern was recorded by using a CCD detector and the X-ray wavelength used was 1.5 Å. (b) Structure factors of the PAM-NP gel studied at different strtching ratios in the direction parallel to stretching.

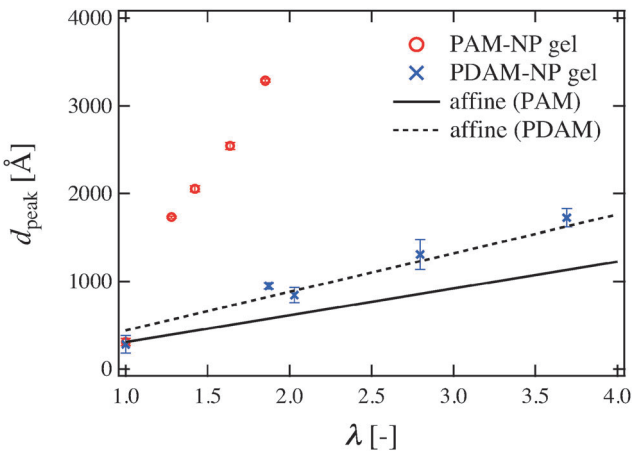

Fig. 4 Stretching ratio dependence of the interparticle distances evaluated from $q_{y,peak}$ in the direction parallel to stretching. The solid and dotted lines shown are theoretical lines calculated for affine deformation in the direction parallel to the stretching for PAM-NP and PDAM-NP gels, respectively.

in the system. Furthermore, we used the y-coordinates of the peaks in the four-spot pattern in the same way as used in the previous studies.[28,29] As shown in Fig. 4, nanoparticles move in an affine way in the case of the PDAM-NP gel. However, in the case of the PAM-NP gel, d_{peak} systematically increases but is remarkably larger than the prediction of affine deformation. This discrepancy cannot be understood if we assume that this peak corresponds to the correlations between the nearest neighbor particles.

In order to understand the origin of this peak, we depicted a schematic illustration of the deformation mechanism inside the PDAM-NP and PAM-NP gels. As shown in Fig. 5, some nanoparticles in the PDAM-NP gel are in direct contact with each other before stretching. When the PDAM-NP gel is uniaxially stretched, nanoparticles which are not in direct contact with each other move in an affine way. On the other hand, in the case of the PAM-NP gel, all nanoparticles are homogeneously dispersed in the system in the unstretched state although there may inherently exist cross-linking heterogeneity in the gel. When the PAM-NP gel is stretched, high cross-linking regions are hardly deformed, while low cross-linking regions are thought to be largely deformed. Thus, the difference in nanoparticle density between high cross-linking regions and low cross-linking regions increases and high cross-linking regions are exaggerated with the increase in the stretching ratio as depicted in Fig. 5. The peaks observed for the PAM-NP gel in our SAXS experiments correspond to the correlation of high-cross-linking density regions.

According to previous works,[17–19,21,22] the introduction of silica nanoparticles into the PAM-NP gel does not lead to any significant effect on the mechanical properties, such as elastic modulus, hysteresis and fracture toughness, while the introduction of silica nanoparticles into the PDAM-NP gel largely increases the mechanical properties of the hydrogel. This difference can be ascribed to the difference in the interaction between polymers and silica nanoparticles. By conducting dynamic light scattering experiments on the NP-loaded P(AM-*co*-DAM) gel, Rose *et al.* showed that there exists an adsorption layer of PDAM onto silica nanoparticles, while no adsorption of PAM occurs.[22] By taking into account these results, each nanoparticle can move in an

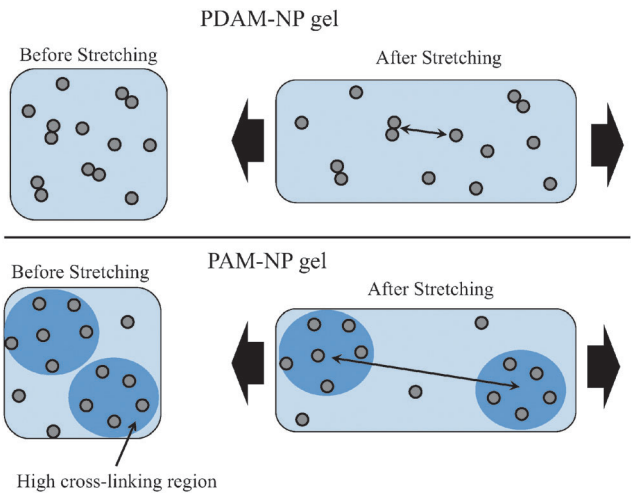

Fig. 5 Schematic images for the stretching mechanism of PDAM-NP and PAM-NP gels. The small circles and large hatched circles denote silica particles and high cross-linking regions, respectively.

affine way when the polymer/filler interaction is strong and polymers chains are adsorbed onto the fillers such as the PDAM-NP gel and ordinary rubber. On the other hand, the cross-linking inhomogeneity can be clearly reflected in the displacements of nanoparticles under stretching when the polymer/filler interaction is weak and polymer chains are not adsorbed on the fillers such as the PAM-NP gel. According to classical theories of rubber elasticity such as an affine model,[31] the magnitude of the deformation of all polymers is assumed to be derived from the macroscopic strain in an affine way. However, the above experimental results clearly indicate that the deformation of polymer strands is more complicated than the assumption of an affine model due to the cross-linking inhomogeneity.

This experimental finding may lead to the establishment of the ''probe-SAXS'' method, which is a method for evaluating cross-linking inhomogeneity in rubbers and gels. Stated in another way, by introducing nanoparticles without disturbing the system, such as local aggregation due to depletion condensation, in the same way as microrheology[7,32,33] and conducting SAXS experiments under uniaxial elongation, we are able to systematically evaluate cross-linking inhomogeneity in the polymeric materials and investigate the correlation between cross-linking inhomogeneity and mechanical properties.

4 Conclusion

We conducted SAXS measurements on PDAM-NP and PAM-NP gels under uniaxial elongation and evaluated 2D structure factors. Interestingly, we found from SAXS measurements that the SAXS scattering profiles of PDAM-NP and PAM-NP gels are totally different. A four-spot pattern was observed for the PDAM-NP gel as in the case of nanocomposite elastomers and rubbers, while sharp peaks were observed in the direction parallel to stretching in the very low-q region for PAM-NP gel. We evaluated stretching ratio dependence of interparticle distances from these scattering peaks and found that nanoparticles in the PDAM-NP gel move in an affine way. However, in the case of the PAM-NP gel, the interparticle distances from scattering peaks are much larger than the theoretical prediction of affine deformation of nanoparticles. This is because the scattering peak in the case of the PAM-NP gel does not correspond to the correlation peak of individual particles but to the correlation peak of the high cross-linking region. In order to test this hypothesis, 2-dimensional pair distribution function analysis and 2-dimensional reverse Monte Carlo simulation must be useful, which will be investigated in our future work.

Acknowledgements

We would like to thank Atsushi Izumi of Advanced Technologies R&D Laboratory, Sumitomo Bakelite Co., Ltd for kind support in SAXS experiments. We also would like to thank Xiang Li, Kazu Hirosawa, and Yasuyuki Shudo of Neutron Science Laboratory, Institute for Solid State Physics, The University of Tokyo for their kind support in SAXS experiments. K. N. acknowledges the support from Research Fellowship for Young Scientists of the Japan Society for the Promotion of Science. The SAXS experiments were performed at the second hutch of SPring-8 BL03XU (Frontier Softmaterial Beamline (FSBL)) constructed by the Consortium of Advanced Softmaterial Beamline and at the BL8S3 beamline at Aichi Synchrotron Radiation Center. We thank Toshihiko Nishida for his useful discussions.

References

1 S. Mallam, F. Horkay, A. M. Hecht and E. Geissler, *Macromolecules*, 1989, **22**, 3356–3361.
2 A. Moussaidt, S. J. Candau and J. G. H. Joosten, *Macromolecules*, 1994, **27**, 2102–2110.
3 M. Shibayama, *Macromol. Chem. Phys.*, 1998, **199**, 1–30.
4 A. Suzuki, M. Yamazaki and Y. Kobiki, *J. Chem. Phys.*, 1996, **104**, 1751–1757.
5 M. Krzeminski, M. Molinari, M. Troyon and X. Coqueret, *Macromolecules*, 2010, **43**, 8121–8127.
6 H. K. Nguyen, M. Ito, S. Fujinami and K. Nakajima, *Macromolecules*, 2014, **47**, 7971–7977.
7 T. G. Mason and D. A. Weitz, *Phys. Rev. Lett.*, 1995, **74**, 1250–1253.
8 M. T. Valentine, P. D. Kaplan, D. Thota, J. C. Crocker, T. Gisler, R. K. Prud'homme, M. Beck and D. A. Weitz, *Phys. Rev. E.*, 2001, **64**, 061506.
9 D. P. P. A. Shundo Jr., K. Matsumoto, M. Ohno, K. Miyaji, M. Goto and K. Tanaka, *Soft Matter*, 2013, **9**, 5166–5172.
10 A. R. Kannurpatti, K. J. Anderson, J. W. Anseth and C. N. Bowman, *J. Polym. Sci. Pt. B Polym. Phys.*, 1997, **35**, 2297–2307.
11 Z. Guo, H. Sautereau and D. E. Kranbuehl, *Macromolecules*, 2005, **38**, 7992–7999.
12 E. Guth, *J. Appl. Phys.*, 1945, **16**, 20–25.
13 L. Petit, L. Bouteiller, A. Brulet, F. Lafuma and D. Hourdet, *Langmuir*, 2007, **78**, 56005–56010.
14 L. S. Schadler, S. C. Giannaris and P. M. Ajayan, *Appl. Phys. Lett.*, 1998, **73**, 3842–3844.
15 P. M. Ajayan, L. S. Schadler, C. Giannaris and A. Rubio, *Adv. Mater.*, 2000, **12**, 750–753.
16 K. Haraguchi and T. Takehisa, *Adv. Mater.*, 2002, **14**, 1120–1124.
17 L. Carlsson, S. Rose, D. Hourdet and A. Marcellan, *Soft Matter*, 2010, **6**, 3619–3631.
18 W. C. Lin, W. Fan, A. Marcellan, D. Hourdet and C. Creton, *Soft Matter*, 2010, **43**, 2554–2563.
19 W. C. Lin, A. Marcellan, D. Hourdet and C. Creton, *Soft Matter*, 2011, **7**, 6578–6582.
20 G. Sudre, D. Hourdet, F. Cousin, C. Creton and Y. Tran, *Langmuir*, 2012, **28**, 12282–12287.
21 S. Rose, A. Dizeux, T. Narita, D. Hourdet and C. Creton, *Macromolecules*, 2013, **46**, 4095–4104.
22 S. Rose, A. Marcellan, D. Hourdet and T. Narita, *Macromolecules*, 2013, **46**, 5329–5336.
23 J. Yang and J. Zhao, *Mater. Lett.*, 2014, **120**, 36–38.
24 L. Ye, Y. Tang and D. Qiu, *Colloids Surf. A*, 2014, **447**, 103–110.

25 A. Guinier and G. Fournet, *Small-Angle Scattering of X-rays.*, Wiley, New York, 1955.
26 D. S. Silvia, *Elementary Scattering Theory: For X-Ray and Neutron Users*, Oxford University Press, New York, 2011.
27 Y. Rharbi, B. Cabane, A. Vacher, M. Joanicot and F. Boue, *Europhys. Lett.*, 1999, **46**, 472–478.
28 Y. Shinohara, H. Kishimoto, K. Inoue, Y. Suzuki, A. Takeuchi, K. Uesugi, N. Yagi, K. Muraoka, T. Mizoguchi and Y. Amemiya, *J. Appl. Cryst.*, 2007, **40**, s397–s401.
29 Y. Ikeda, Y. Yasuda, S. Yamamoto and Y. Morita, *J. Appl. Cryst.*, 2007, **40**, s549–s552.
30 J. Oberdisse, *Soft Matter*, 2006, **2**, 29–36.
31 P. J. Flory, *Principles of Polymer Chemistry*, Cornell University Press, Ithaca and NY and London, 1953.
32 F. Gittes, B. Schnurr, P. D. Olmsted, F. C. MacKintosh and C. F. Schmidt, *Phys. Rev. Lett.*, 1997, **79**, 3286–3289.
33 B. Schnurr, F. Gittes, F. C. MacKintosh and C. F. Schmidt, *Macromolecules*, 1997, **30**, 7781–7792.